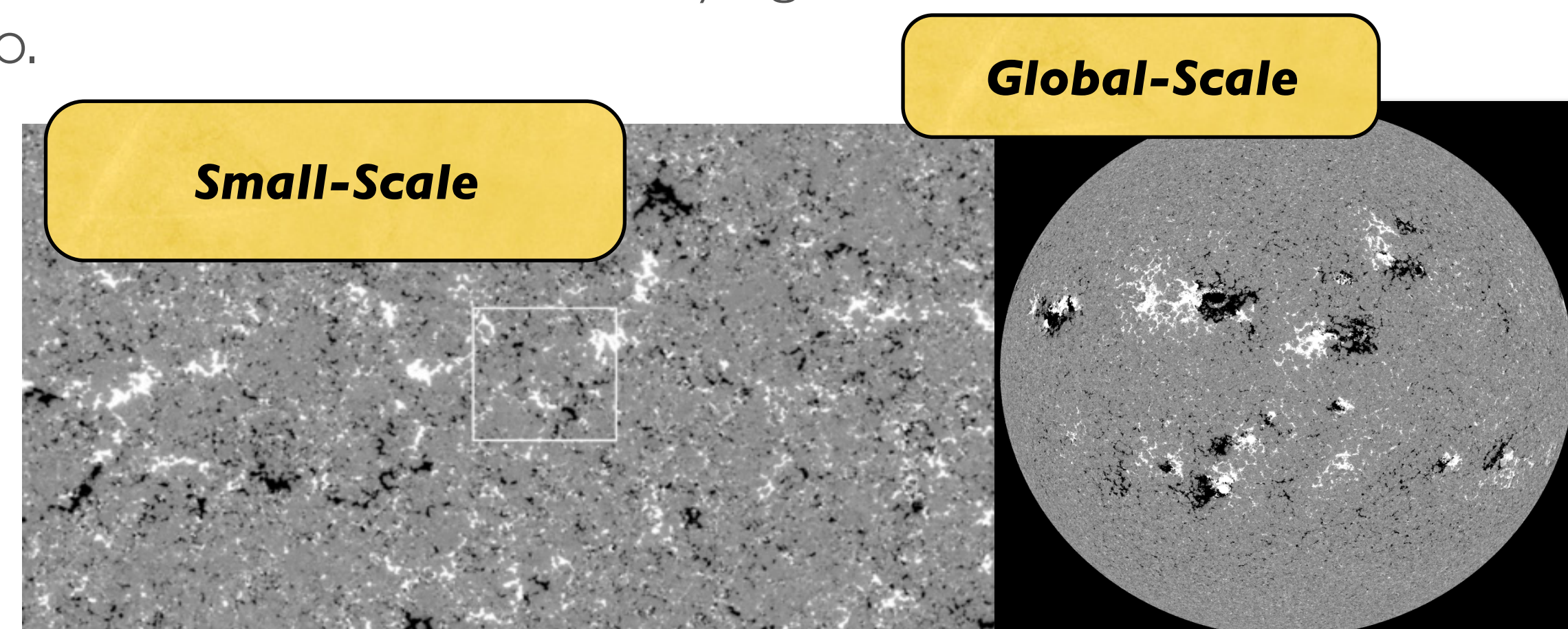
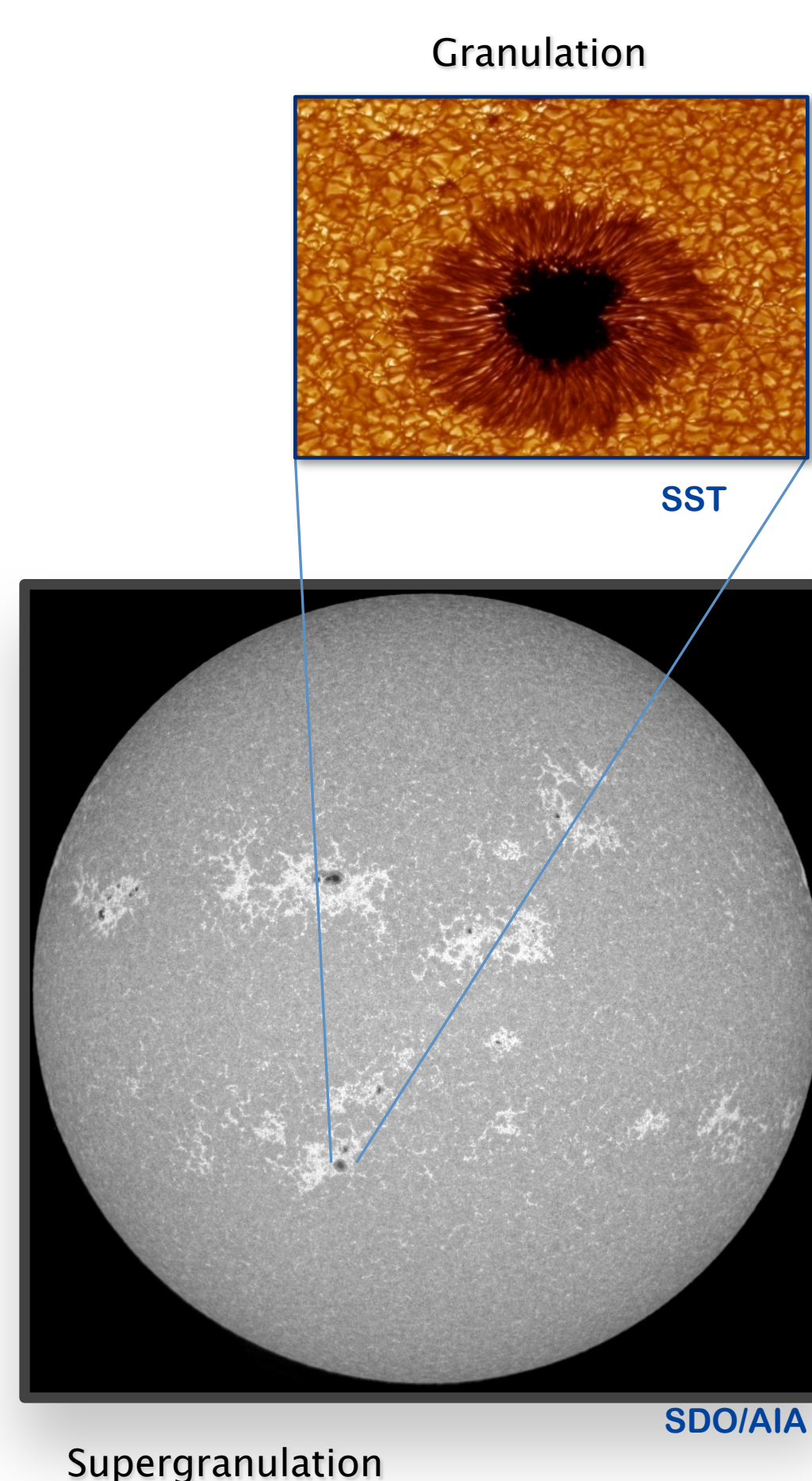


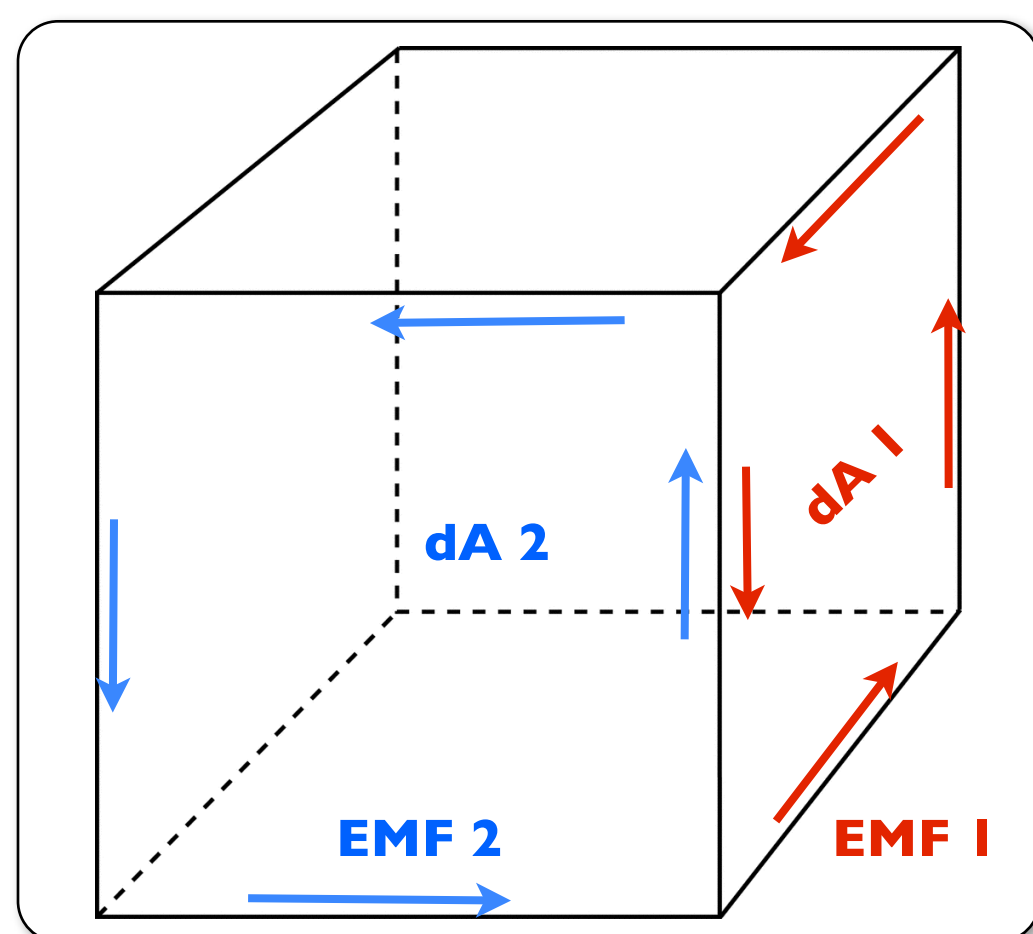
## 1. Motivation

Convection and magnetic fluctuations in the sun exist on many scales. There are granules and super granules which result in up and down flows in different regions and on different length scales. In addition there are large sunspots as well as much smaller magnetic field variations that appear near the surface. In addition to all of this the sun varies over a 22 year period. Capturing all of these length and time scales in one model is nearly impossible and it is important to understand what limitations we are imposing on our models when we try to do so. My work looks at magnetic field in a variety of flow patterns to understand how the field behaves as well as what limitations are imposed upon it in the form of numerical diffusion. These simulations were done in 2 and 3 dimensions and in situations with both a decaying field and a dynamo.



## 2. Methodology

The computational domain is broken up into many small cubes. EMF through each face is calculated and cancellation between cell faces results in no net flux (constrained transport). Magnetostatics preserves divergence free magnetic field by integrating EMF around cell faces



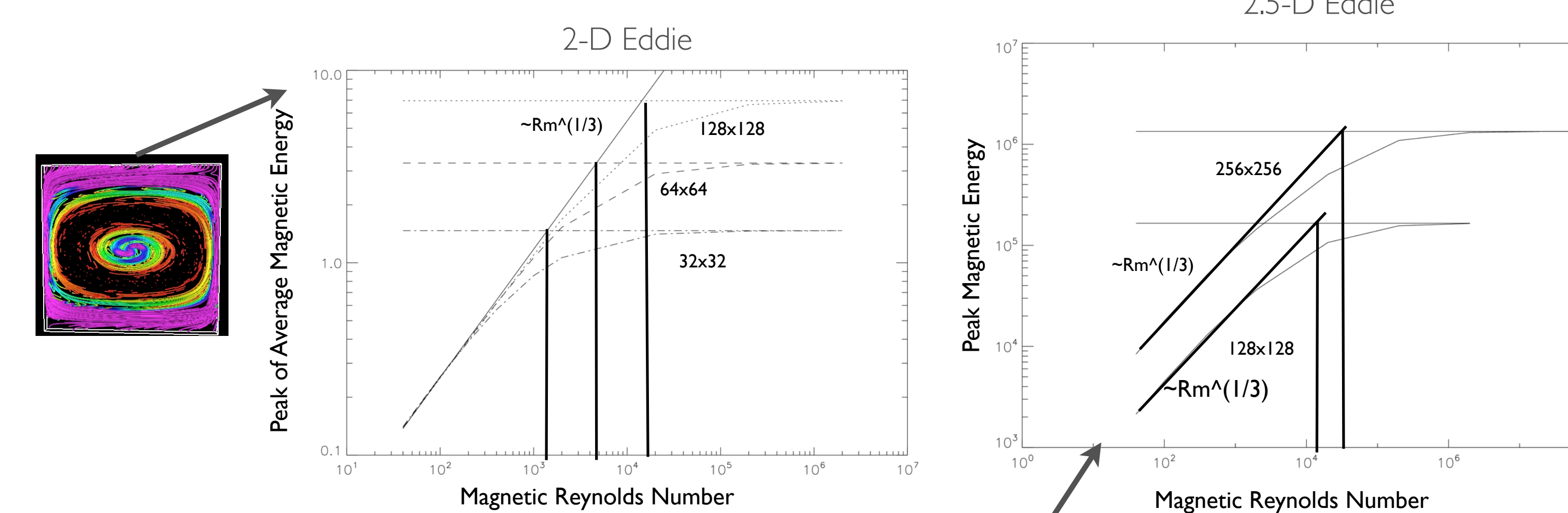
## The Induction Equation

$$\frac{\partial \mathbf{B}}{\partial t} = \underbrace{\nabla \times (\mathbf{v} \times \mathbf{B})}_{\text{Generation}} + \underbrace{\eta \nabla^2 \mathbf{B}}_{\text{Dissipation}}$$

$$\nabla \times (\mathbf{v} \times \mathbf{B}) = \underbrace{\mathbf{v}(\nabla \cdot \mathbf{B})}_{\text{Always zero}} - \underbrace{\mathbf{B}(\nabla \cdot \mathbf{v})}_{\text{Compression and Expansion}} + \underbrace{(\mathbf{B} \cdot \nabla) \mathbf{v}}_{\text{Stretching and Shear}} - \underbrace{\mathbf{v} \cdot \nabla \mathbf{B}}_{\text{Advection (Movement)}}$$

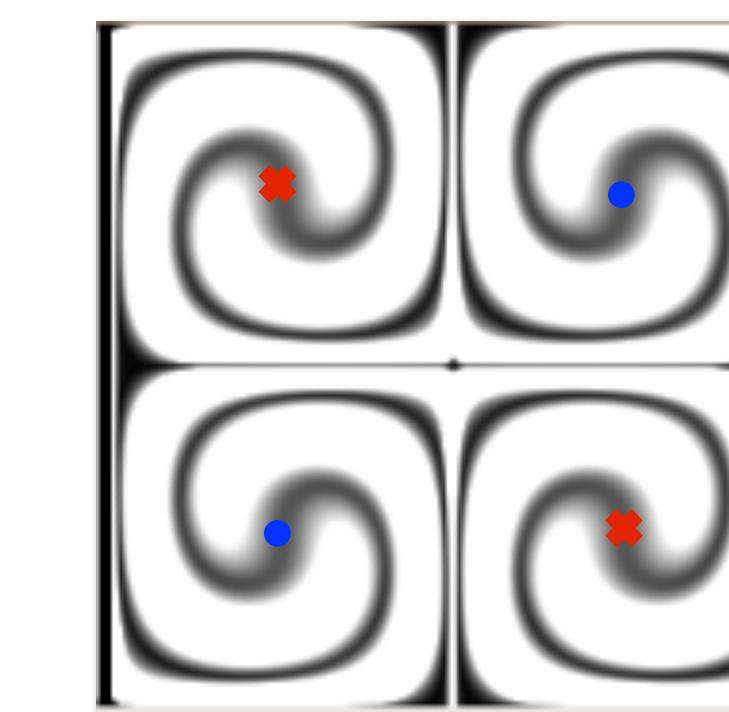
## 3. Results

In order to calculate the numerical diffusion the same simulation was run repeatedly with an imposed diffusion that started out large and approached zero. As the diffusion was lowered the peak magnetic energy would increase. However because there was always a numerical diffusion in place the peak would approach a limit. Because the expected solution of this process is known (it goes like the magnetic Reynolds number to the 1/3) I was able to plot the magnetic Reynolds number vs peak magnetic energy on a log/log scale. From the parts with high imposed diffusion a fit was calculated. The point where this fit (linear on the graph) reached the value of the peak with no imposed diffusion would give the inherent magnetic Reynolds number, and therefore the numerical diffusion. Included here are the graphs of this process for two different field types.



$$\begin{aligned} v_x^a &= A \sin\left(\frac{2\pi x}{L_x}\right) \cos\left(\frac{2\pi y}{L_y}\right) \\ v_y^a &= -A \cos\left(\frac{2\pi x}{L_x}\right) \sin\left(\frac{2\pi y}{L_y}\right) \\ v_z^a &= \sin\left(\frac{2\pi x}{L_x}\right) \sin\left(\frac{2\pi y}{L_y}\right), \end{aligned}$$

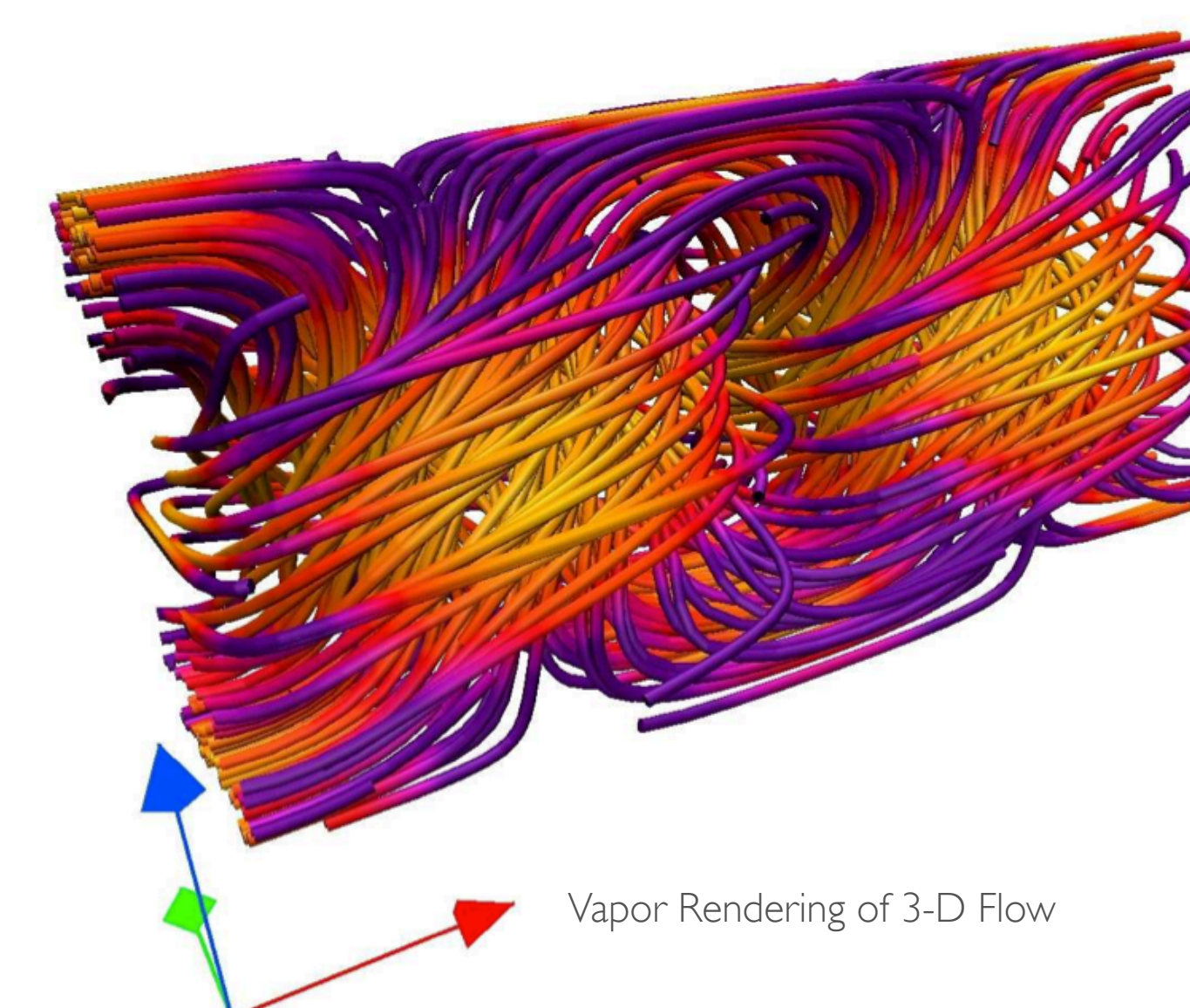
- Invariant in z-direction
- Vortices do not connect



- Into Slide
- Out of Slide

## 4. Results

After analyzing decaying flows a new 3-D flow equation was written with the goal of creating a dynamo. We were successful and a vapor rendering of the flow as well as the equation is included here. The equation for the flow is a weighted sum of two different flows that resulted in multiple vortices in the x-y plane and that had flows coming up out of or down into their centers. The flow created a buildup of magnetic energy around the edges of the vortices and the magnetic energy grew exponentially over a hundred thousand iterations.



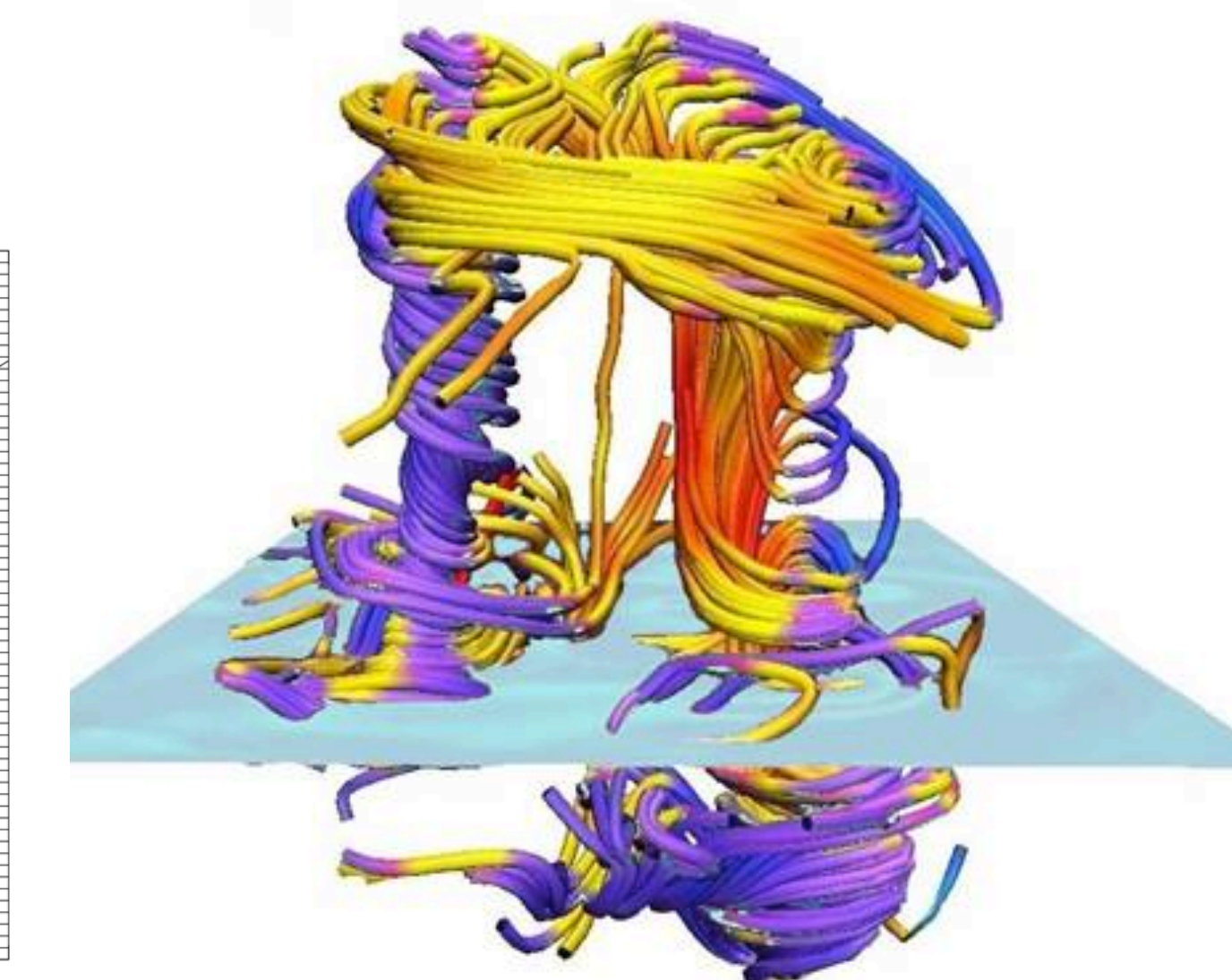
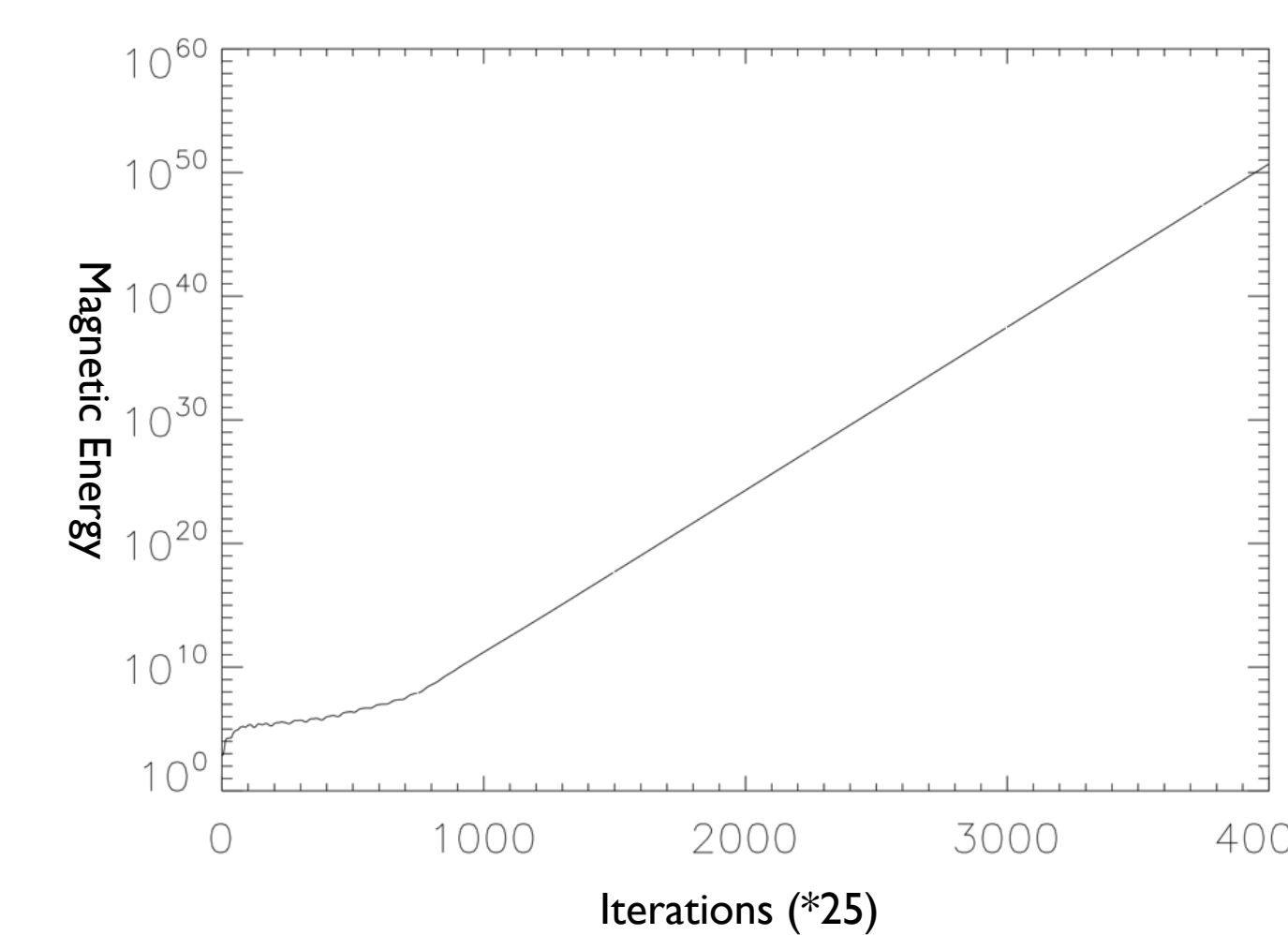
### A-flow

$$\begin{aligned} v_x^a &= A \sin\left(\frac{2\pi x}{L_x}\right) \cos\left(\frac{2\pi y}{L_y}\right) \\ v_y^a &= -A \cos\left(\frac{2\pi x}{L_x}\right) \sin\left(\frac{2\pi y}{L_y}\right) \\ v_z^a &= \sin\left(\frac{2\pi x}{L_x}\right) \sin\left(\frac{2\pi y}{L_y}\right), \end{aligned}$$

### B-flow

$$\begin{aligned} v_x^b &= \cos\left(\frac{2\pi x}{L_x}\right) \sin\left(\frac{2\pi y}{L_y}\right) \cos\left(\frac{2\pi z}{L_z}\right) \\ v_y^b &= 0 \\ v_z^b &= \sin\left(\frac{2\pi x}{L_x}\right) \sin\left(\frac{2\pi y}{L_y}\right) \sin\left(\frac{2\pi z}{L_z}\right). \end{aligned}$$

### Fully 3-D Dynamo



Example of a flow in current stellar models  
Featherstone et al 2009

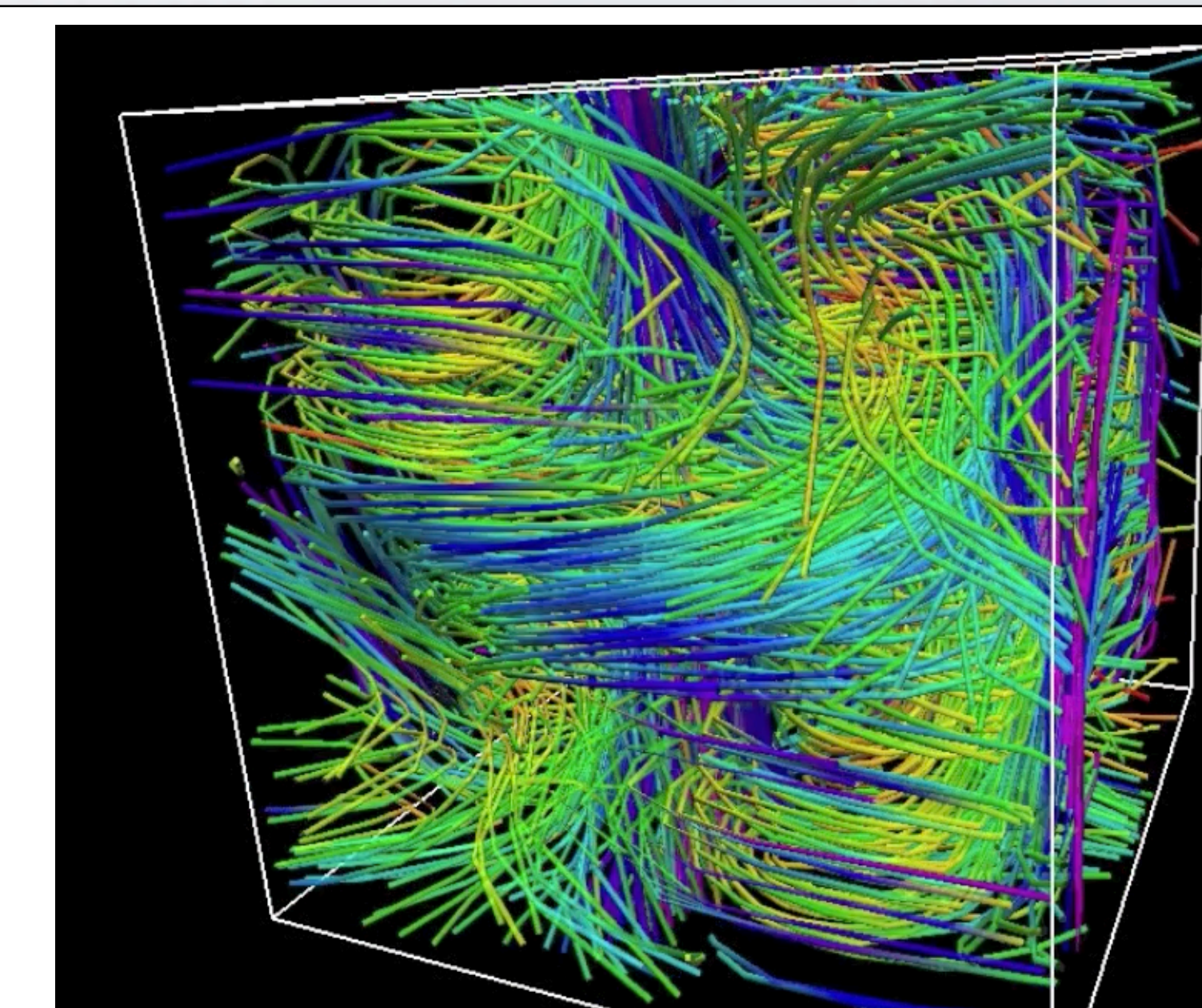
Total flow is a weighted sum of the two

$$\mathbf{v} = (1 - w(z))\mathbf{v}^a + w(z)\mathbf{v}^b,$$

$$w(z) = \frac{1}{2} \left( 1 + \cos\left(\frac{4\pi z}{L_z}\right) \right).$$

## 5. Conclusions

The two dimensional flows with known analytic solutions validated the code and allowed us to analyze the numerical diffusion. From this we saw that as the grid spacing doubles the numerical diffusion was roughly cut in half. Applying this same process to a 3-D flow whose magnetic energy eventually decayed showed that while the numerical diffusion changed with the flow, the effect of changing the grid resolution remained the same. We found that our solar-motivated 3-D flow was capable of sustaining a dynamo. Although new methods would be needed to assess the numerical diffusion in this situation it is achievable with current methods and would provide insight into the numerical diffusion present in larger models of the sun. Finally, we note that our idealized 3-D flow does not encapsulate the effects of meridional circulation and differential rotation. We plan to extend these studies to examine their effects.



Vapor Rendering of Magnetic Field Lines in 3-D Flow